Published in final edited form as:
*J Immunol*. 2012 December 1; 189(11): 5129–5138. doi:10.4049/jimmunol.1201570.

# ATP-Binding Cassette Transporter G1 Intrinsically Regulates Invariant NKT Cell Development

**Duygu Sag**[*], **Gerhard Wingender**[†], **Heba Nowyhed**[*], **Runpei Wu**[*], **Abraham K. Gebre**[‡], **John S. Parks**[‡], **Mitchell Kronenberg**[†], and **Catherine C. Hedrick**[*]

[*]Division of Inflammation Biology, La Jolla Institute for Allergy and Immunology, La Jolla, CA 92037

[†]Division of Developmental Immunology, La Jolla Institute for Allergy and Immunology, La Jolla, CA 92037

[‡]Department of Pathology/Lipid Sciences and Biochemistry, Wake Forest University School of Medicine, Winston-Salem, NC 27157

## Abstract

ATP-binding cassette transporter G1 (ABCG1) plays a role in the intracellular transport of cholesterol. Invariant NKT (*i*NKT) cells are a subpopulation of T lymphocytes that recognize glycolipid Ags. In this study, we demonstrate that ABCG1 regulates *i*NKT cell development and functions in a cell-intrinsic manner. *Abcg1*$^{-/-}$ mice displayed reduced frequencies of *i*NKT cells in thymus and periphery. Thymic *i*NKT cells deficient in ABCG1 had reduced membrane lipid raft content, and showed impaired proliferation and defective maturation during the early stages of development. Moreover, we found that *Abcg1*$^{-/-}$ mice possess a higher frequency of V$\beta7^{+}$ *i*NKT cells, suggesting alterations in *i*NKT cell thymic selection. Furthermore, in response to CD3ε/CD28 stimulation, *Abcg1*$^{-/-}$ thymic *i*NKT cells showed reduced production of IL-4 but increased production of IFN-γ. Our results demonstrate that changes in intracellular cholesterol homeostasis by ABCG1 profoundly impact *i*NKT cell development and function.

Natural killer T cells are a unique subset of T lymphocytes that share characteristics with both NK cells and conventional T cells. There are two main classes of NKT cells, type I and type II. Type I NKT cells, also referred to as invariant NKT (*i*NKT) cells, express an invariant TCR (*i*TCR) α-chain, utilizing Vα14Jα18 in mice and Vα24Jα18 in humans. This *i*TCR α-chain is paired with a limited TCRβ chain repertoire, predominantly Vβ8, Vβ7, or Vβ2 in mice, and Vβ11 in humans (1). Unlike conventional MHC class I- and class II-reactive T cells, which recognize peptide Ags, *i*NKT cells recognize glycolipid Ags presented by CD1d, a MHC class I-like molecule (1). At least two classes of glycolipids have been reported to bear antigenic activity for *i*NKT cells, as follows: glycosphingolipids, as exemplified by Ags found in *Sphingomonas* bacteria (2, 3), and diacylglycerols, found, for example, in *Borrelia* bacteria (4). There are reports that other types of lipids, including cholesterol-containing molecules from *Helicobacter pylori*, are recognized by *i*NKT cells (5). The best-studied Ag for *i*NKT cells is the glycosphingolipid, α-galactosylceramide (α-GalCer) (6). Upon activation with α-GalCer, *i*NKT cells are able to produce large quantities of both Th1 cytokines (IFN-γ) and Th2 cytokines (IL-4, IL-10, and IL-13) (7, 8). Thus,



Address correspondence and reprint requests to Prof. Catherine C. Hedrick, Division of Inflammation Biology, La Jolla Institute for Allergy and Immunology, 9420 Athena Circle, La Jolla, CA 92037. hedrick@liai.org.

Disclosures
The authors have no financial conflicts of interest.

*i*NKT cells can modulate immunity in a broad range of diseases and conditions, including atherosclerosis, autoimmunity, cancer, diabetes, allergy, and infection (7, 8).

ATP-binding cassette (ABC) transporters are transmembrane proteins that facilitate the transport of specific substrates across the membrane in an ATP-dependent manner (9). ABC transporter G1 (ABCG1) is a member of the ABC transporter family that regulates cholesterol homeostasis in the cell (10). Cholesterol homeostasis is crucial for the growth and survival of cells, because cholesterol is a key component of cell membranes and lipid rafts (11). ABCG1 is expressed in many tissues, including spleen, brain, lung, and kidney, and in many cell types, including lymphocytes, myeloid cells, and endothelial cells (12). Whereas ABCG1 can localize to the plasma membrane, it resides mostly intracellularly. Although initial studies suggested that the main function of ABCG1, similar to the other cholesterol transporter ABC transporter A1 (ABCA1), is to promote cholesterol efflux from cells (12, 13), recent reports by us and others show that ABCG1 is also important for the intracellular transport of cholesterol (14, 15). We previously reported that ABCG1 regulates the transfer of cholesterol from outer to inner membrane leaflets in secretory granules, including insulin granules in the pancreas (14). A recent study by Tarling and Edwards (15) has demonstrated that ABCG1 localizes to endocytic vesicles to facilitate the redistribution of intracellular cholesterol away from the endoplasmic reticulum. Thus, a key function of ABCG1 may be to regulate membrane cholesterol content to facilitate proper membrane fluidity and cholesterol homeostasis.

ABCG1 expression in immune cells, such as macrophages and lymphocytes, impacts their function. ABCG1-deficient macrophages display increased inflammatory activity (16, 17) in response to LPS (18), and when loaded with cholesterol (19). We (20) and others (21) have reported that changes in cholesterol and lipid raft content in the absence of ABCG1 increase TCR signaling and proliferation of $CD4^+$ T cells. Like other lymphocytes, *i*NKT cells express ABCG1; however, the role of ABCG1 and cholesterol homeostasis in *i*NKT cell biology is not known. In this study, we demonstrate that changes in intracellular cholesterol homeostasis by ABCG1 profoundly impact thymic *i*NKT cell development and function.

## Materials and Methods

### Mice

C57BL/6J mice (000664) and B6.129S7-$Rag1^{tm1Mom}$/J (002216) mice were purchased from The Jackson Laboratory (Bar Harbor, ME). *Abcg1*$^{-/-}$/*lacZ* knock-in mice were purchased from Deltagen (San Mateo, CA) and are congenic on a C57BL/6J background. B6.SJL-Ptprca/BoyAiTac mice (CD45.1 congenic, 004007) were purchased from Taconic Farms (Germantown, NY). Mice were fed a standard rodent chow diet and were housed in microisolator cages in a pathogen-free animal facility of the La Jolla Institute for Allergy and Immunology. All experiments followed guidelines of the La Jolla Institute for Allergy and Immunology Animal Care and Use Committee, and approval for use of rodents was obtained from the La Jolla Institute for Allergy and Immunology according to criteria outlined in the *Guide for the Care and Use of Laboratory Animals* from the National Institutes of Health. Mice were euthanized by $CO_2$ inhalation.

### Reagents

Flow cytometry Abs, including anti-mouse CD45.2 (104), CD4 (RM4-5), TCRβ (H57-597), IL-4 (BVD6-24G2), CD44 (IM7), NK1.1 (PK136), and CD1d (1B1), were purchased from eBioscience (San Diego, CA); CD45.1 (A20), IFN-γ (XMG1.2), Vβ7 (TR310), and Vβ8.1/2 (MR5-2) were purchased from BD Biosciences (San Jose, CA); CD19 (6D5) and CD8α (5H10) were purchased from Invitrogen (Carlsbad, CA); Vβ2 (B20.6) was purchased from

BioLegend (San Diego, CA); and neuropilin-1 (NRP-1) (polyclonal) was purchased from R&D Systems (Minneapolis, MN). Allophycocyanin-conjugated CD1d tetramers loaded with PBS-57 (an α-GalCer analog) were provided by the National Institutes of Health Tetramer Facility. PE and Pacific blue-conjugated α-GalCer–loaded CD1d tetramers were produced, as previously described (22). Anti-CD3ε (145-2C11), anti-CD28 (37.51), and CD16/CD32 (2.4G2) Abs were purchased from BD Biosciences. RPMI 1640 medium was purchased from Invitrogen (Carlsbad, CA), and PBS was purchased from Thermo Scientific (Rockford, IL).

### Primary cell preparation

Single-cell suspensions were prepared from the thymus, spleen, and liver. Spleens and thymi were meshed through a 40-μm strainer (Fisher Scientific, Pittsburgh, PA). RBCs in spleen were lysed in RBC lysis buffer, according to the manufacturer's protocol (BioLegend). Prior to extraction, the liver was perfused with PBS via the portal vein until opaque and meshed through a 100-μm strainer and washed. Total liver cells were then resus-pended in a 37.5% isotonic Percoll solution (Amersham Biosciences, Piscataway, NJ) and centrifuged for 30 min at 850 × *g* at room temperature. After centrifugation, RBCs were lysed, as described above.

### Flow cytometry

Cells were resuspended in 100 μl flow cytometry staining buffer (1% BSA plus 0.1% sodium azide in PBS). FcRγ were blocked with CD16/32 blocking Ab for 10 min, and surface Ags on cells were stained for 30 min at 4°C. Cells were stained with the CD1d tetramer together with the other surface Abs in staining buffer. LIVE/DEAD Fixable Dead Cell Stain (Invitrogen) was used for analysis of viability, and forward- and side-scatter parameters were used for exclusion of doublets from analysis. Ab clones used are listed above.

For measurement of membrane lipid rafts, cells were stained for an additional 10 min at 4°C in PBS with 10 ng Alexa-Fluor 488-labeled cholera toxin B (CT-B) from Vybrant lipid-raft labeling kits (Invitrogen).

For intracellular staining, cells were fixed and permeabilized with the Cytofix/Cytoperm Fixation/Permeabilization Solution Kit (BD Biosciences) after the cell surface staining. Cells were stained for 30 min at 4°C with directly conjugated fluorescent of IL-4 and IFN-γ Abs.

Calculations of percentages were based on live cells as determined by forward- and side-scatter and viability analysis. Cell fluorescence was assessed using LSR-II (BD Biosciences), and data were analyzed with FlowJo software (Tree Star, Ashland, OR).

### In vitro stimulation assays

For activation of *i*NKT cell hybridomas, $5 \times 10^4$ *i*NKT cell hybridoma DN3A4-1.2 cells were cultured with $5 \times 10^5$ thymocytes in the presence of titrated amounts of α-GalCer (1.6, 6.3, 25, 100, 400 ng/ml) in 96-well plates in vitro. After 18 h, IL-2 levels in the supernatant were quantitated using a mouse IL-2 ELISA kit (eBioscience), according to the manufacturer's instructions. For activation of primary *i*NKT cells, 24-well plates were coated with 5 μg/ml αCD3ε Ab in PBS at 4°C overnight. The next day, the plates were washed twice with PBS, and thymocytes were plated at $2 \times 10^6$ cells/well in RPMI 1640 medium supplemented with 5% FBS and 1% penicillin/streptomycin. Soluble αCD28 Ab (2 μg/ml) and GolgiPlug (BD Biosciences) were added, and the cells were incubated at 37°C for 4 h. Thymocytes were stimulated with PMA (1 μg/ml) and ionomycin (200 ng/ml) for 4

h in the presence of GolgiPlug at 37°C. IL-4 and IFN-γ production by *i*NKT cells was assessed by flow cytometry.

### In vivo BrdU proliferation assay and detection of apoptosis

C57BL/6 (B6) and *Abcg1*$^{-/-}$ mice were injected i.p. with 0.3 mg BrdU (in 100 μl PBS) three times every 4 h. Thymi were harvested the next day, and single-cell suspensions were stained with fluorophore-conjugated Abs and CD1d tetramer. After cell surface staining, cells were analyzed for BrdU incorporation using FITC or allophycocyanin BrdU flow kit (BD Biosciences), according to the manufacturer's instructions. Apoptosis of thymic *i*NKT cells was measured by flow cytometry using a PE Annexin V Apoptosis Detection Kit 1 (BD Biosciences), according to the manufacturer's instructions.

### Generation of bone marrow chimeras

Recipient mice (Rag1$^{-/-}$) were irradiated in two doses of 450 rad each (for a total of 900 rad) 4 h apart. Bone marrow cells from both femurs and tibias of donor mice (B6.SJL and *Abcg1*$^{-/-}$) were collected under sterile conditions. Bones were centrifuged for the collection of marrow, and cells were washed, mixed at 1:1 ratio, and resuspended in PBS for injection. Approximately $5 \times 10^6$ bone marrow cells from B6.SJL and *Abcg1*$^{-/-}$ mice (total $10^7$ cells) in 200 μl PBS were delivered retro-orbitally into each recipient mouse. Recipient mice were housed in a barrier facility under pathogen-free conditions before and after bone marrow transplantation. After bone marrow transplantation, mice were provided autoclaved acidified water with antibiotics (trimethoprim-sulfamethoxazole) and were fed autoclaved food. Mice were analyzed 12 wk after bone marrow reconstitution.

### Cholesterol content in iNKT cells

Surface Ags on thymocytes from B6 and *Abcg1*$^{-/-}$ mice were stained, as described above, followed by *i*NKT cell (CD8$^-$, TCRβ$^+$, CD1d tetramer$^+$) sorting with a FACSAria cytometer (BD Biosciences). Approximately $2 \times 10^5$ events were collected for gas chromatography analysis. Sorted thymic *i*NKT cells were pelleted by low-spin centrifugation. After several washes with PBS, the cell pellet was extracted with chloroform:methanol (2:1) containing 5-cholestane as internal standard. Total and free cholesterol content was determined by gas–liquid chromatography and normalized to cellular protein, as previously described (23). Cholesteryl ester was calculated as (total cholesterol – free cholesterol) × 1.67. Multiplying by 1.67 corrects for the average fatty acid mass that is lost during saponification.

### Quantitative real-time PCR

*i*NKT cells were FACS sorted from thymus, and total cellular RNA was collected with an RNeasy Plus Micro Kit, according to the manufacturer's protocol (Qiagen, Valencia, CA). RNA purity and quantity were measured with a nanodrop spectrophotometer (Thermo Scientific). Approximately 500 ng RNA was used for synthesis of cDNA with an Iscript cDNA Synthesis Kit (Bio-Rad, Hercules, CA). Total cDNA was diluted 1:20 in $H_2O$, and a volume of 9 μl was used for each real-time condition with a MyIQ Single-Color Real-Time PCR Detection System (Bio-Rad) and TaqMan Gene Expression Mastermix and ABCG1 and ABCA1 TaqMan primers (Invitrogen). Data were analyzed and presented on the basis of the relative expression method (24). The formula for this calculation is as follows: relative expression = $2^{-(S\Delta Ct - C\Delta Ct)}$ where $\Delta C_t$ is the difference in the threshold cycle between the gene of interest and the housekeeping gene (18S), S is the *Abcg1*$^{-/-}$ mouse, and C is the B6 control mouse.

### Statistical analysis

Data for all experiments were analyzed with Prism software (GraphPad, San Diego, CA). Unpaired Student *t* test was used for comparison of experimental groups. The $p$ values $<0.05$ were considered statistically significant.

## Results

### Abcg1$^{-/-}$ mice display impaired iNKT cell development

To investigate the impact of ABCG1 deficiency on *i*NKT cell development, *i*NKT cell frequencies in thymus, liver, and spleen of four- to six-week-old *Abcg1*$^{-/-}$ and control B6 mice were assessed by flow cytometry (Fig. 1A, 1B). *Abcg1*$^{-/-}$ mice had significantly lower frequencies of *i*NKT cells in both thymus and liver compared with control mice (Fig. 1A, 1B). Absolute cell numbers of *i*NKT cells in thymus and liver were also lower in *Abcg1*$^{-/-}$ mice compared with control mice (Fig. 1C). A similar tendency was observed in the spleen; however, this did not reach statistical significance in all experiments (Fig. 1A–C). Recently, Milpied et al. (25) reported that recent thymic emigrant *i*NKT cells express NRP-1 and lack CD69. To determine whether the *Abcg1*$^{-/-}$ mice had impaired export of *i*NKT cells from thymus, we examined the expression of NRP-1 and CD69 in splenic *i*NKT cells of *Abcg1*$^{-/-}$ and control mice. As shown in Fig. 1D, the frequency of NRP-1$^{+}$CD69$^{-}$ *i*NKT cells in spleen of *Abcg1*$^{-/-}$ mice was significantly lower compared with control mice. Overall, these data suggest that ABCG1 deficiency reduces the production and thymic egress of *i*NKT cells.

*i*NKT cells can be divided into CD4$^{+}$ and CD4$^{-}$ subsets, and into subpopulations that express NK1.1, which is associated with functional differences (26). We therefore measured expression of CD4 and NK1.1 on *i*NKT cells in thymus and spleen of *Abcg1*$^{-/-}$ mice and B6 control mice by flow cytometry. We did not observe any differences in the percentages of these phenotypic *i*NKT cell subsets in either organ (Supplemental Fig. 1).

The invariant Vα14Jα18 TCR chain of *i*NKT cells is paired with a restricted set of β-chains containing mainly Vβ8.1/2, Vβ7, and Vβ2, with diverse CDR3 regions (1). There are data suggesting that Vβ7$^{+}$ *i*NKT cells have a higher affinity for the endogenous ligand(s) presented during positive selection of *i*NKT cells in the thymus (27). Thus, the frequency of Vβ7$^{+}$ *i*NKT cells has been used as a surrogate marker for the overall avidity for the *i*TCR toward its endogenous selecting ligand(s) in the thymus. To determine whether ABCG1 deficiency could impact the selection of *i*NKT cells in the thymus, we first analyzed Vβ7$^{+}$ *i*NKT cells in *Abcg1*$^{-/-}$ mice. As shown in Fig. 1E, the percentages of Vβ7$^{+}$ *i*NKT cells in thymus, liver, and spleen of *Abcg1*$^{-/-}$ mice were significantly higher than in the control B6 mice. Next, we analyzed Vβ8.1/2$^{+}$ and Vβ2$^{+}$ *i*NKT cells in these organs and found that in thymus and spleen of *Abcg1*$^{-/-}$ mice, the percentages of Vβ8.1/2$^{+}$ and Vβ2$^{+}$ *i*NKT cells were significantly lower than in the B6 mice, which is in line with the increased frequency of Vβ7$^{+}$ *i*NKT cells in the *Abcg1*$^{-/-}$ mice (Fig. 1E). In liver, the percentage of Vβ8.1/2$^{+}$ *i*NKT cells was significantly lower in *Abcg1*$^{-/-}$ mice compared with B6 mice; however, the percentages of Vβ2$^{+}$ *i*NKT cells in *Abcg1*$^{-/-}$ mice and B6 mice were comparable (Fig. 1E). Next, we determined the absolute cell numbers of Vβ7$^{+}$ *i*NKT cells in *Abcg1*$^{-/-}$ mice. In line with the reduced total *i*NKT cell frequency in thymus of *Abcg1*$^{-/-}$ mice compared with control B6 mice (Fig. 1A, 1B), the absolute cell number of Vβ7$^{+}$ *i*NKT cells in thymus was also significantly lower in *Abcg1*$^{-/-}$ mice (Fig. 1F). In liver, the absolute cell number of Vβ7$^{+}$ *i*NKT cells tended to be lower in *Abcg1*$^{-/-}$ mice, but the difference was not statistically significant ($p = 0.067$) (Fig. 1F). As the frequencies of total *i*NKT cells in spleen of *Abcg1*$^{-/-}$ mice and B6 mice were comparable (Fig. 1A, 1B) and *Abcg1*$^{-/-}$ mice had a higher percentage of Vβ7$^{+}$ *i*NKT cells in spleen (Fig. 1E), the absolute cell numbers of

Vβ7$^+$ *i*NKT cells in spleen were significantly higher in *Abcg1*$^{-/-}$ mice (Fig. 1F). These data demonstrate that thymic selection of Vβ7$^+$ *i*NKT cells is favored in the absence of ABCG1.

## ABCG1 deficiency affects iNKT cell development via a cell-intrinsic mechanism

A critical factor driving *i*NKT cell development in the thymus is the generation of a CD1d-restricted *i*TCR by CD4$^+$CD8$^+$ double-positive (DP) cortical thymocytes (28, 29). Once a DP thymocyte expressing an *i*TCR interacts with a CD1d-expressing DP cortical thymocyte that presents endogenous selecting ligand(s), the *i*TCR-expressing DP thymocyte is positively selected to enter the thymic *i*NKT cell precursor pool (30). Subsequently, these *i*NKT cell precursors undergo a series of proliferation and differentiation/maturation stages (31). Because *i*NKT cells are positively selected by DP thymocytes, we examined whether DP thymocytes from *Abcg1*$^{-/-}$ mice had lower CD1d expression. If so, this would be a likely explanation for the observed decrease in *i*NKT cell frequency. As shown in Fig. 2A, DP thymocytes from *Abcg1*$^{-/-}$ and B6 mice had similar levels of surface CD1d expression. Next, to investigate whether ABCG1 deficiency affects CD1d-mediated lipid Ag presentation, we incubated the *i*NKT cell hybridoma DN3A4-1.2 with thymocytes isolated from either *Abcg1*$^{-/-}$ or B6 mice in the presence of titrated amounts of α-GalCer in vitro. We found that *Abcg1*$^{-/-}$ thymocytes were as efficient as B6 thymocytes at stimulating IL-2 production by *i*NKT cell hybridomas (Fig. 2B). Overall, these results show that the impairment in *i*NKT cell development observed in *Abcg1*$^{-/-}$ mice was not due to changes in CD1d surface expression on DP thymocytes or their CD1d-mediated Ag presentation.

To determine whether the impact of ABCG1 deficiency on *i*NKT cell development is mediated through cell-intrinsic factor(s), we used a mixed bone marrow chimera approach. Irradiated Rag1$^{-/-}$ mice were reconstituted with both CD45.1$^+$ B6.SJL and CD45.2$^+$ *Abcg1*$^{-/-}$ bone marrow mixed at a 1:1 ratio and analyzed 12 wk after reconstitution. We did not observe any difference in the frequency of *Abcg1*$^{-/-}$ and B6 DP thymocytes (Supplemental Fig. 2A) or in their surface CD1d expression in the chimeric mice (Supplemental Fig. 2B). However, when analyzing *i*NKT cells in the thymus, we found that ~3-fold fewer *i*NKT cells developed from the *Abcg1*$^{-/-}$ bone marrow than from the B6 bone marrow (Fig. 2C, 2D). These results demonstrate that the impact of ABCG1 deficiency on *i*NKT cell development in the thymus is cell intrinsic.

To determine whether the increased frequency of Vβ7$^+$ *i*NKT cells in *Abcg1*$^{-/-}$ mice (Fig. 1E) was also caused by a cell-intrinsic mechanism, we evaluated the percentage of Vβ7$^+$ *i*NKT cells in the 1:1 mixed bone marrow chimeric mice. *Abcg1*$^{-/-}$-derived *i*NKT cells in the thymus of the chimeric mice displayed a higher frequency of Vβ7$^+$ population compared with B6-derived *i*NKT cells (Fig. 2E). These data demonstrate that thymic selection of Vβ7$^+$ *i*NKT cells is favored in the absence of ABCG1 via an *i*NKT cell-intrinsic mechanism.

## ABCG1 deficiency affects the maturation of iNKT cells in the thymus

After positive selection in thymus, *i*NKT cells proliferate and differentiate/mature along stages that are defined by the surface expression of CD44 and NK1.1 (31). Cells with a stage 1 phenotype (CD44$^{low}$ NK1.1$^-$) are followed by stage 2 cells, which have increased CD44 expression (CD44$^{high}$ NK1.1$^-$). Stage 1 and stage 2 *i*NKT cells are highly proliferative (32, 33). The upregulation of NK1.1 expression by *i*NKT cells marks stage 3 (CD44$^{high}$ NK1.1$^+$) cells, which are mature but less proliferative (32, 34). Whereas most *i*NKT cells exit the thymus at stage 2 and complete their maturation in the periphery, some enter stage 3 in the thymus and remain as long-term thymus-resident *i*NKT cells (31). To determine where during *i*NKT cell development ABCG1 plays a role, we evaluated the developmental stages of *i*NKT cells in the 1:1 mixed bone marrow chimeric mice. The percentage of

*Abcg1*$^{-/-}$ *i*NKT cells in stage 1 (CD44$^{low}$ NK1.1$^{2}$) was ~2-fold larger compared with B6 *i*NKT cells, whereas the percentage of *i*NKT cells in stage 2 (CD44$^{high}$ NK1.1$^{-}$) was reduced by 33%. There were no differences in the percentages of stage 3 (CD44$^{high}$ NK1.1$^{+}$) *i*NKT cells between both genotypes (Fig. 3A, 3B). We calculated the absolute cell numbers of *Abcg1*$^{-/-}$ and B6 *i*NKT cells at these three maturation stages, and, in line with the reduced relative frequency of *Abcg1*$^{-/-}$ *i*NKT cells in the thymus of the chimeric mice (Fig. 2C, 2D), the total number of *Abcg1*$^{-/-}$ *i*NKT cells was dramatically reduced at stages 2 and 3 compared with B6 *i*NKT cells (Fig. 3C). Subsequently, we analyzed Vβ7$^{+}$ *i*NKT cells in stage 1–3 of thymic development in *Abcg1*$^{-/-}$ mice. Similar to the observed increase in the frequency of total thymic Vβ7$^{+}$ *i*NKT cells in *Abcg1*$^{-/-}$ mice (Fig. 1E), the frequencies of Vβ7$^{+}$ *i*NKT cells in all three maturation stages were significantly higher in *Abcg1*$^{-/-}$ mice than in B6 mice (Fig. 3D). These data indicate that ABCG1 deficiency impairs the proper maturation of *i*NKT cells at early stages of *i*NKT cell development.

## Abcg1$^{-/-}$ iNKT cells have reduced proliferation

To determine whether the reduced frequency of *i*NKT cells in the absence of ABCG1 is due to a decrease in proliferation, we measured proliferation of thymic *i*NKT cells at different maturation stages in vivo in *Abcg1*$^{-/-}$ and B6 control mice by BrdU incorporation. In *Abcg1*$^{-/-}$ mice, the frequency of BrdU$^{+}$ *i*NKT cells at stages 1 and 2 was significantly reduced compared with *i*NKT cells from B6 mice (Fig. 4A, 4B). In stage 3, the frequency of BrdU$^{+}$ *i*NKT cells also tended to be lower in *Abcg1*$^{-/-}$ mice, but the difference was not statistically significant ($p = 0.051$) (Fig. 4A, 4B). Next, we measured BrdU incorporation of Vβ7$^{+}$ *i*NKT cells in *Abcg1*$^{-/-}$ and B6 mice. In line with the reduced proliferation of total *i*NKT cells in *Abcg1*$^{-/-}$ mice (Fig. 4A, 4B), the frequency of BrdU$^{+}$ Vβ7$^{+}$ *i*NKT cells was significantly lower in *Abcg1*$^{-/-}$ mice compared with B6 mice (Supplemental Fig. 4). To investigate whether increased cell death also contributes to the reduced *i*NKT cell numbers in the absence of ABCG1, we examined apoptosis of *Abcg1*$^{-/-}$ and B6 *i*NKT cells at different stages of thymic development by annexin V staining. We found that the percentages of apoptotic (annexin V$^{+}$ live) *i*NKT cells at stage 1–3 in *Abcg1*$^{-/-}$ and B6 mice were comparable (Fig. 4C, 4D). These results indicate that the reduced frequency of *i*NKT cells in thymus in the absence of ABCG1 is not due to increased cell death but reduced proliferation, particularly during the early stages of development.

## ABCG1 deficiency affects lipid raft content in iNKT cells

We next measured the cholesterol content in *i*NKT cells isolated from thymus of B6 and *Abcg1*$^{-/-}$ mice using gas chromatography. We found no significant changes in the cholesteryl ester, free cholesterol, or total cholesterol content in *Abcg1*$^{-/-}$ *i*NKT cells (Fig. 5A). However, as ABCG1 is important in intracellular cholesterol transport (14, 15) and cholesterol is an important component of membrane lipid rafts (11), we measured lipid raft content in thymic *i*NKT cells. Lipid rafts are specialized regions of the cell membrane that are rich in cholesterol and gangliosides and act as platforms to colocalize proteins involved in intracellular signaling pathways (35, 36). In contrast to the comparable cholesterol levels, the lipid raft content of *Abcg1*$^{-/-}$ *i*NKT cells in thymus was 43% lower than in B6 *i*NKT cells (Fig. 5B, 5C). These results suggest that ABCG1 plays a role in regulation of membrane lipid raft content in thymic *i*NKT cells, which is most likely important for their proper development.

## ABCG1 deficiency affects cytokine production of iNKT cells

Because *Abcg1*$^{-/-}$ *i*NKT cells have reduced lipid raft content (Fig. 5B, 5C) and the TCR is associated with lipid rafts (37), we next investigated whether deficiency of ABCG1 in *i*NKT cells would affect their TCR-driven activation. We stimulated thymocytes from B6:*Abcg1*$^{-/-}$ 1:1 mixed bone marrow chimeric mice with plate-bound aCD3ε and soluble

costimulatory αCD28 Ab in vitro and measured IL-4 and IFN-γ production of thymic *i*NKT cells by intracellular staining. We found that CD45.2$^+$ *Abcg1*$^{-/-}$ *i*NKT cells had reduced IL-4 production, but enhanced IFN-γ production compared with CD45.1$^+$ B6 *i*NKT cells (Fig. 6A, 6B). Previous studies have shown that stage 1 and stage 2 *i*NKT cells produce abundant IL-4, but less IFN-γ, whereas stage 3 *i*NKT cells make more IFN-γ, but less IL-4 (32, 34, 38). Our results demonstrate that the frequency and the total cell number of stage 2 *i*NKT cells are reduced in the absence of ABCG1 (Fig. 3A–C). Therefore, the diminished production of IL-4 by *Abcg1*$^{-/-}$ *i*NKT cells might be due to the lower percentages of the potent IL-4 producer stage 2 *i*NKT cells in the absence of ABCG1. To address this possibility, we stimulated thymocytes from *Abcg1*$^{-/-}$ and B6 mice with αCD3ε and αCD28 Abs in vitro and measured IL-4 and IFN-γ production of thymic *i*NKT at different stages by intracellular staining. Stage 2 and stage 3 *Abcg1*$^{-/-}$ *i*NKT cells produced significantly less IL-4 and more IFN-γ compared with B6 control (Fig. 6C), demonstrating that the altered cytokine production of *Abcg1*$^{-/-}$ *i*NKT cells is not due to the reduced percentages of stage 2 *i*NKT cells in the absence of ABCG1. Furthermore, to elucidate that the changes in the cytokine production by *i*NKT cells in the absence of ABCG1 are related to TCR triggering, we stimulated thymocytes from *Abcg1*$^{-/-}$ and B6 mice in vitro with PMA/ionomycin, which bypasses TCR triggering to induce activation. We then measured IL-4 and IFN-γ production of thymic *i*NKT cells by intracellular staining. As seen in Fig. 6D, PMA/ionomycin stimulation induced IL-4 and IFN-γ production by *Abcg1*$^{-/-}$ *i*NKT cells to a similar degree as in the B6 *i*NKT cells, indicating that Th1-biased cytokine production we observed in *Abcg1*$^{-/-}$ *i*NKT cells is indeed related to TCR triggering. Overall, these results demonstrate that deficiency of ABCG1 in *i*NKT cells skews their cytokine production, leading to a Th1 bias following TCR-driven activation.

## Discussion

In this study, we demonstrate that changes in cholesterol homeostasis caused by the absence of ABCG1 impair *i*NKT cell development. ABCG1-deficient thymic *i*NKT cells displayed reduced proliferation in vivo and defective maturation during the early stages of development. Considering the number of thymic *i*NKT cells, the developmental block was particularly evident at stage 2, although the reduced proliferation of stage 1 cells most likely contributes to the deficit. Moreover, in the absence of ABCG1, thymic *i*NKT cells had reduced membrane lipid raft content, which was accompanied by a Th1-biased cytokine production in response to TCR stimulation. The defects were cell intrinsic, meaning that they occur in the *i*NKT cell precursor rather than in the DP thymocyte responsible for *i*NKT cell-positive selection. Therefore, although it is theoretically possible that a cholesterol-containing compound is an important self-ligand mediating positive selection, our results rule out differences in self-ligand presentation as the responsible factor. In addition, thymic selection of Vβ7$^+$ *i*NKT cells was favored in the absence of ABCG1 via an *i*NKT cell-intrinsic mechanism. Importantly, to our knowledge, our work illustrates for the first time an *i*NKT cell-intrinsic modulation of the TCR Vβ repertoire during thymic selection. Furthermore, to our knowledge, our work is the first to demonstrate that changes in intracellular cholesterol homeostasis profoundly impact *i*NKT cell development and function.

We (20) and Bensinger et al. (21) have previously reported that alterations in intracellular cholesterol homeostasis in the absence of ABCG1 lead to a hyperproliferative phenotype of conventional T cells. In our previous study, we showed that ABCG1-deficient CD4$^+$ T cells displayed enhanced TCR signaling and proliferation as a result of increased cholesterol and lipid raft content (20). In contrast, this study reveals an opposite role of ABCG1 in *i*NKT cells, as ABCG1-deficient *i*NKT cells displayed decreased proliferation and lower membrane lipid raft content. *i*NKT cells differ from naive CD4$^+$ T cells in that they have an activated/memory phenotype and they produce large amounts of both Th1 and Th2

cytokines following activation with glycolipid Ags (8). Therefore, it is plausible that *i*NKT cells have differences in cholesterol metabolism and, as such, different requirements for cholesterol homeostasis than do $CD4^+$ T cells. Excess cholesterol is exported out of the cell by the cholesterol transporters ABCA1 and ABCG1 (39, 40). ABCA1 effluxes cholesterol to lipid-poor apolipoprotein AI (41), whereas ABCG1 promotes cholesterol efflux to mature high-density lipoprotein particles (13). *i*NKT cells express both ABCG1 and ABCA1 (Supplemental Fig. 3A, 3B). ABCA1 expression is enhanced in *Abcg1*$^{-/-}$ *i*NKT cells compared with B6 *i*NKT cells (Supplemental Fig. 3B). This is not surprising, because many previous studies have shown that genetic deletion of one cholesterol transporter, either ABCA1 or ABCG1, is compensated for by an upregulation of the other transporter (20, 42, 43). Nonetheless, neither ABCA1 nor ABCG1 can fully compensate for the loss of the other (10). However, we cannot rule out the possibility that changes in ABCA1 expression contributed to our observed findings of altered *i*NKT cell development and function in *Abcg1*$^{-/-}$ mice. Whereas, in the absence of ABCG1, the total cholesteryl ester content of $CD4^+$ T cells increases (20), the total cholesteryl ester of *i*NKT cells is unchanged (Fig. 5A). These results suggest that, in terms of regulating cholesteryl ester content, ABCA1 can substitute for the lack of ABCG1 in *i*NKT cells, but not in T cells. Future studies of the role of ABCA1 in *i*NKT cells using floxed mice may be useful to delineate the different roles of these two transporters in *i*NKT cell development.

Apart from cholesterol efflux, ABCG1 is also important for intracellular cholesterol transport (14, 15). Cholesterol is an essential component of membrane lipid rafts (11). Because *i*NKT cells have a reduction in the lipid raft content (Fig. 5B, 5C) without any changes in the overall cholesterol content (Fig. 5A) in the absence of ABCG1, the critical role of ABCG1 in *i*NKT cells seems to be the regulation of the intracellular transport of cholesterol. Miguel et al. (44) have recently shown that the amount of membrane lipid rafts present in $CD4^+$ T cells correlates closely with immunological synapse formation and $CD4^+$ T cell proliferation and activation. Therefore, based on our data, we hypothesize that ABCG1 deficiency causes a decrease in the transport of cholesterol to the cell membrane, affecting lipid rafts, which impacts *i*NKT cell development and function.

Our results demonstrate that, in the absence of ABCG1, thymic selection of $V\beta7^+$ *i*NKT cells is favored in a cell-intrinsic manner. Previous studies have shown that $V\beta7^+$ *i*NKT cells have a lower affinity toward α-GalCer (45), whereas, based on the analysis of $CD1d^{+/-}$ heterozygous mice, they may have a higher affinity for the endogenous ligand(s) for the positive selection of *i*NKT cells in thymus (27). Therefore, the frequency of thymic $V\beta7^+$ *i*NKT cells may be a surrogate marker for the overall avidity of the *i*TCR toward its endogenous selecting ligand(s) in the thymus. In previous studies, which showed that the thymic selection of the $V\beta7^+$ *i*NKT cells was favored, the reduced avidity of the *i*TCR toward the selecting ligand(s) was due to reduced expression of CD1d on DP thymocytes (27). However, in our study, the surface expression levels of CD1d on DP thymocytes in *Abcg1*$^{-/-}$ mice were unchanged (Fig. 2A). Furthermore, the expression levels of the TCR/CD3 complex were similar in the *Abcg1*$^{-/-}$ *i*NKT cells compared with control mice (data not shown). As the effects we observed were *i*NKT cell intrinsic (Fig. 2E), this altogether suggests that the differences in the avidity of the *i*TCR–CD1d interaction in the *Abcg1*$^{-/-}$ mice are due to changes in the *i*TCR itself. Based on our data, we hypothesize that the alterations in the lipid raft content in the absence of ABCG1 modify the distribution of the TCR in *i*NKT cells so that it is less colocalized in lipid rafts. These changes may make the *i*TCR less sensitive to the endogenous ligand(s) presented by CD1d for the positive selection of *i*NKT cells in thymus. Such a reduction may favor the selection of relatively high-affinity $V\beta7^+$ *i*NKT cells in the thymus and lead to reduced export of *i*NKT cells to the periphery. Changes in the composition/organization of the *i*TCR also alter cytokine production of

*i*NKT cells. More work is needed, however, to examine how ABCG1 deficiency leads to a Th1-biased cytokine production.

In summary, we demonstrate a novel role for ABCG1-mediated cholesterol homeostasis in *i*NKT cell development. *i*NKT cells have been implicated in the development of atherosclerosis, rheumatoid arthritis, several forms of allergy, as well as autoimmunity (7, 8). All of these diseases have known or proposed lipid constituents that increase risk of disease development. For example, ABCG1-deficient (43, 46), as well as *i*NKT cell-deficient mice are protected from atherosclerosis development (47–51). Therefore, linking the role of lipid transporters and glycolipid-sensitive *i*NKT cells could lead to the development of entirely new therapeutic approaches for diseases that have a hyperlipidemic component, such as atherosclerosis.

## Supplementary Material

Refer to Web version on PubMed Central for supplementary material.

## Acknowledgments

We thank Amy Blatchley, Archana Khurana, the Department of Laboratory Animal Care, and the flow cytometry facility at the La Jolla Institute for Allergy and Immunology for excellent technical assistance. We also thank Dr. Isaac Engel and Dr. Meng Zhao for valuable scientific contributions.

This work was supported by National Institutes of Health Grants R01 HL097368 and R01 HL085790 (to C.C.H.), R01 HL094525 (to J.S.P.), and RO1 AI45053 and R37 AI71922 (to M.K.).

## Abbreviations used in this article

| | |
|---|---|
| **ABC** | ATP-binding cassette |
| **ABCA1** | ABC transporter A1 |
| **ABCG1** | ABC transporter G1 |
| **CT-B** | cholera toxin B |
| **DP** | double-positive |
| **α-GalCer** | α-galactosylceramide |
| ***i*NKT** | invariant NKT |
| ***i*TCR** | invariant TCR |
| **NRP-1** | neuropilin-1 |

## References

1. Godfrey DI, MacDonald HR, Kronenberg M, Smyth MJ, Van Kaer L. NKT cells: what's in a name? Nat. Rev. Immunol. 2004; 4:231–237. [PubMed: 15039760]
2. Kinjo Y, Wu D, Kim G, Xing GW, Poles MA, Ho DD, Tsuji M, Kawahara K, Wong CH, Kronenberg M. Recognition of bacterial glycosphingolipids by natural killer T cells. Nature. 2005; 434:520–525. [PubMed: 15791257]
3. Mattner J, Debord KL, Ismail N, Goff RD, Cantu C III, Zhou D, Saint-Mezard P, Wang V, Gao Y, Yin N, et al. Exogenous and endogenous glycolipid antigens activate NKT cells during microbial infections. Nature. 2005; 434:525–529. [PubMed: 15791258]
4. Kinjo Y, Tupin E, Wu D, Fujio M, Garcia-Navarro R, Benhnia MR, Zajonc DM, Ben-Menachem G, Ainge GD, Painter GF, et al. Natural killer T cells recognize diacylglycerol antigens from pathogenic bacteria. Nat. Immunol. 2006; 7:978–986. [PubMed: 16921381]

5. Chang YJ, Kim HY, Albacker LA, Lee HH, Baumgarth N, Akira S, Savage PB, Endo S, Yamamura T, Maaskant J, et al. Influenza infection in suckling mice expands an NKT cell subset that protects against airway hyperreactivity. J. Clin. Invest. 2011; 121:57–69. [PubMed: 21157038]
6. Kawano T, Cui J, Koezuka Y, Toura I, Kaneko Y, Motoki K, Ueno H, Nakagawa R, Sato H, Kondo E, et al. CD1d-restricted and TCR-mediated activation of Valpha14 NKT cells by glycosylceramides. Science. 1997; 278:1626–1629. [PubMed: 9374463]
7. Bendelac A, Savage PB, Teyton L. The biology of NKT cells. Annu. Rev. Immunol. 2007; 25:297–336. [PubMed: 17150027]
8. Godfrey DI, Kronenberg M. Going both ways: immune regulation via CD1d-dependent NKT cells. J. Clin. Invest. 2004; 114:1379–1388. [PubMed: 15545985]
9. Higgins CF. ABC transporters: from microorganisms to man. Annu. Rev. Cell Biol. 1992; 8:67–113. [PubMed: 1282354]
10. Tarr PT, Tarling EJ, Bojanic DD, Edwards PA, Baldán A. Emerging new paradigms for ABCG transporters. Biochim. Biophys. Acta. 2009; 1791:584–593. [PubMed: 19416657]
11. Ikonen E. Cellular cholesterol trafficking and compartmentalization. Nat. Rev. Mol. Cell Biol. 2008; 9:125–138. [PubMed: 18216769]
12. Kennedy MA, Barrera GC, Nakamura K, Baldán A, Tarr P, Fishbein MC, Frank J, Francone OL, Edwards PA. ABCG1 has a critical role in mediating cholesterol efflux to HDL and preventing cellular lipid accumulation. Cell Metab. 2005; 1:121–131. [PubMed: 16054053]
13. Wang N, Lan D, Chen W, Matsuura F, Tall AR. ATP-binding cassette transporters G1 and G4 mediate cellular cholesterol efflux to high-density lipoproteins. Proc. Natl. Acad. Sci. USA. 2004; 101:9774–9779. [PubMed: 15210959]
14. Sturek JM, Castle JD, Trace AP, Page LC, Castle AM, Evans-Molina C, Parks JS, Mirmira RG, Hedrick CC. An intracellular role for ABCG1-mediated cholesterol transport in the regulated secretory pathway of mouse pancreatic beta cells. J. Clin. Invest. 2010; 120:2575–2589. [PubMed: 20530872]
15. Tarling EJ, Edwards PA. ATP binding cassette transporter G1 (ABCG1) is an intracellular sterol transporter. Proc. Natl. Acad. Sci. USA. 2011; 108:19719–19724. [PubMed: 22095132]
16. Baldán A, Gomes AV, Ping P, Edwards PA. Loss of ABCG1 results in chronic pulmonary inflammation. J. Immunol. 2008; 180:3560–3568. [PubMed: 18292583]
17. Wojcik AJ, Skaflen MD, Srinivasan S, Hedrick CC. A critical role for ABCG1 in macrophage inflammation and lung homeostasis. J. Immunol. 2008; 180:4273–4282. [PubMed: 18322240]
18. Yvan-Charvet L, Welch C, Pagler TA, Ranalletta M, Lamkanfi M, Han S, Ishibashi M, Li R, Wang N, Tall AR. Increased inflammatory gene expression in ABC transporter-deficient macrophages: free cholesterol accumulation, increased signaling via Toll-like receptors, and neutrophil infiltration of atherosclerotic lesions. Circulation. 2008; 118:1837–1847. [PubMed: 18852364]
19. Yvan-Charvet L, Ranalletta M, Wang N, Han S, Terasaka N, Li R, Welch C, Tall AR. Combined deficiency of ABCA1 and ABCG1 promotes foam cell accumulation and accelerates atherosclerosis in mice. J. Clin. Invest. 2007; 117:3900–3908. [PubMed: 17992262]
20. Armstrong AJ, Gebre AK, Parks JS, Hedrick CC. ATP-binding cassette transporter G1 negatively regulates thymocyte and peripheral lymphocyte proliferation. J. Immunol. 2010; 184:173–183. [PubMed: 19949102]
21. Bensinger SJ, Bradley MN, Joseph SB, Zelcer N, Janssen EM, Hausner MA, Shih R, Parks JS, Edwards PA, Jamieson BD, Tontonoz P. LXR signaling couples sterol metabolism to proliferation in the acquired immune response. Cell. 2008; 134:97–111. [PubMed: 18614014]
22. Matsuda JL, Naidenko OV, Gapin L, Nakayama T, Taniguchi M, Wang CR, Koezuka Y, Kronenberg M. Tracking the response of natural killer T cells to a glycolipid antigen using CD1d tetramers. J. Exp. Med. 2000; 192:741–754. [PubMed: 10974039]
23. Rudel LL, Kelley K, Sawyer JK, Shah R, Wilson MD. Dietary monounsaturated fatty acids promote aortic atherosclerosis in LDL receptor-null, human ApoB100-overexpressing transgenic mice. Arterioscler. Thromb. Vasc. Biol. 1998; 18:1818–1827. [PubMed: 9812923]
24. Livak KJ, Schmittgen TD. Analysis of relative gene expression data using real-time quantitative PCR and the 2(-Delta Delta C(T)) method. Methods. 2001; 25:402–408. [PubMed: 11846609]

25. Milpied P, Massot B, Renand A, Diem S, Herbelin A, Leite-de-Moraes M, Rubio MT, Hermine O. IL-17-producing invariant NKT cells in lymphoid organs are recent thymic emigrants identified by neuropilin-1 expression. Blood. 2011; 118:2993–3002. [PubMed: 21653940]
26. Coquet JM, Chakravarti S, Kyparissoudis K, McNab FW, Pitt LA, McKenzie BS, Berzins SP, Smyth MJ, Godfrey DI. Diverse cytokine production by NKT cell subsets and identification of an IL-17-producing CD42K1.12 NKT cell population. Proc. Natl. Acad. Sci. USA. 2008; 105:11287–11292. [PubMed: 18685112]
27. Schümann J, Mycko MP, Dellabona P, Casorati G, MacDonald HR. Cutting edge: influence of the TCR Vbeta domain on the selection of semi-invariant NKT cells by endogenous ligands. J. Immunol. 2006; 176:2064–2068. [PubMed: 16455960]
28. Bendelac A. Positive selection of mouse NK1+ T cells by CD1-expressing cortical thymocytes. J. Exp. Med. 1995; 182:2091–2096. [PubMed: 7500054]
29. Gapin L, Matsuda JL, Surh CD, Kronenberg M. NKT cells derive from double-positive thymocytes that are positively selected by CD1d. Nat. Immunol. 2001; 2:971–978. [PubMed: 11550008]
30. Kronenberg M, Engel I. On the road: progress in finding the unique pathway of invariant NKT cell differentiation. Curr. Opin. Immunol. 2007; 19:186–193. [PubMed: 17303398]
31. Godfrey DI, Stankovic S, Baxter AG. Raising the NKT cell family. Nat. Immunol. 2010; 11:197–206. [PubMed: 20139988]
32. Benlagha K, Kyin T, Beavis A, Teyton L, Bendelac A. A thymic precursor to the NK T cell lineage. Science. 2002; 296:553–555. [PubMed: 11968185]
33. Benlagha K, Wei DG, Veiga J, Teyton L, Bendelac A. Characterization of the early stages of thymic NKT cell development. J. Exp. Med. 2005; 202:485–492. [PubMed: 16087715]
34. Pellicci DG, Hammond KJ, Uldrich AP, Baxter AG, Smyth MJ, Godfrey DI. A natural killer T (NKT) cell developmental pathway involving a thymus-dependent NK1.1(–)CD4(+) CD1d-dependent precursor stage. J. Exp. Med. 2002; 195:835–844. [PubMed: 11927628]
35. Brown DA, London E. Functions of lipid rafts in biological membranes. Annu. Rev. Cell Dev. Biol. 1998; 14:111–136. [PubMed: 9891780]
36. Simons K, Toomre D. Lipid rafts and signal transduction. Nat. Rev. Mol. Cell Biol. 2000; 1:31–39. [PubMed: 11413487]
37. Jury EC, Flores-Borja F, Kabouridis PS. Lipid rafts in T cell signalling and disease. Semin. Cell Dev. Biol. 2007; 18:608–615. [PubMed: 17890113]
38. Gadue P, Stein PL. NK T cell precursors exhibit differential cytokine regulation and require Itk for efficient maturation. J. Immunol. 2002; 169:2397–2406. [PubMed: 12193707]
39. Gelissen IC, Harris M, Rye KA, Quinn C, Brown AJ, Kockx M, Cartland S, Packianathan M, Kritharides L, Jessup W. ABCA1 and ABCG1 synergize to mediate cholesterol export to apoA-I. Arterioscler. Thromb. Vasc. Biol. 2006; 26:534–540. [PubMed: 16357317]
40. Vaughan AM, Oram JF. ABCA1 and ABCG1 or ABCG4 act sequentially to remove cellular cholesterol and generate cholesterol-rich HDL. J. Lipid Res. 2006; 47:2433–2443. [PubMed: 16902247]
41. Vedhachalam C, Duong PT, Nickel M, Nguyen D, Dhanasekaran P, Saito H, Rothblat GH, Lund-Katz S, Phillips MC. Mechanism of ATP-binding cassette transporter A1-mediated cellular lipid efflux to apolipoprotein A-I and formation of high density lipoprotein particles. J. Biol. Chem. 2007; 282:25123–25130. [PubMed: 17604270]
42. Brunham LR, Kruit JK, Pape TD, Timmins JM, Reuwer AQ, Vasanji Z, Marsh BJ, Rodrigues B, Johnson JD, Parks JS, et al. Beta-cell ABCA1 influences insulin secretion, glucose homeostasis and response to thiazolidinedione treatment. Nat. Med. 2007; 13:340–347. [PubMed: 17322896]
43. Ranalletta M, Wang N, Han S, Yvan-Charvet L, Welch C, Tall AR. Decreased atherosclerosis in low-density lipoprotein receptor knockout mice transplanted with Abcg1$^{-/-}$ bone marrow. Arterioscler. Thromb. Vasc. Biol. 2006; 26:2308–2315. [PubMed: 16917103]
44. Miguel L, Owen DM, Lim C, Liebig C, Evans J, Magee AI, Jury EC. Primary human CD4+ T cells have diverse levels of membrane lipid order that correlate with their function. J. Immunol. 2011; 186:3505–3516. [PubMed: 21307290]

45. Schümann J, Voyle RB, Wei BY, MacDonald HR. Cutting edge: influence of the TCR V beta domain on the avidity of CD1d:alpha-galactosylceramide binding by invariant V alpha 14 NKT cells. J. Immunol. 2003; 170:5815–5819. [PubMed: 12794105]

46. Baldán A, Pei L, Lee R, Tarr P, Tangirala RK, Weinstein MM, Frank J, Li AC, Tontonoz P, Edwards PA. Impaired development of atherosclerosis in hyperlipidemic Ldlr$^{-/-}$ and ApoE$^{-/-}$ mice transplanted with Abcg1$^{-/-}$ bone marrow. Arterioscler. Thromb. Vasc. Biol. 2006; 26:2301–2307. [PubMed: 16888235]

47. Aslanian AM, Chapman HA, Charo IF. Transient role for CD1d-restricted natural killer T cells in the formation of atherosclerotic lesions. Arterioscler. Thromb. Vasc. Biol. 2005; 25:628–632. [PubMed: 15591216]

48. Major AS, Wilson MT, McCaleb JL, Ru Su Y, Stanic AK, Joyce S, Van Kaer L, Fazio S, Linton MF. Quantitative and qualitative differences in proatherogenic NKT cells in apolipoprotein E-deficient mice. Arterioscler. Thromb. Vasc. Biol. 2004; 24:2351–2357. [PubMed: 15472130]

49. Nakai Y, Iwabuchi K, Fujii S, Ishimori N, Dashtsoodol N, Watano K, Mishima T, Iwabuchi C, Tanaka S, Bezbradica JS, et al. Natural killer T cells accelerate atherogenesis in mice. Blood. 2004; 104:2051–2059. [PubMed: 15113755]

50. Rogers L, Burchat S, Gage J, Hasu M, Thabet M, Willcox L, Ramsamy TA, Whitman SC. Deficiency of invariant V alpha 14 natural killer T cells decreases atherosclerosis in LDL receptor null mice. Cardiovasc. Res. 2008; 78:167–174. [PubMed: 18192239]

51. Tupin E, Nicoletti A, Elhage R, Rudling M, Ljunggren HG, Hansson GK, Berne GP. CD1d-dependent activation of NKT cells aggravates atherosclerosis. J. Exp. Med. 2004; 199:417–422. [PubMed: 14744994]

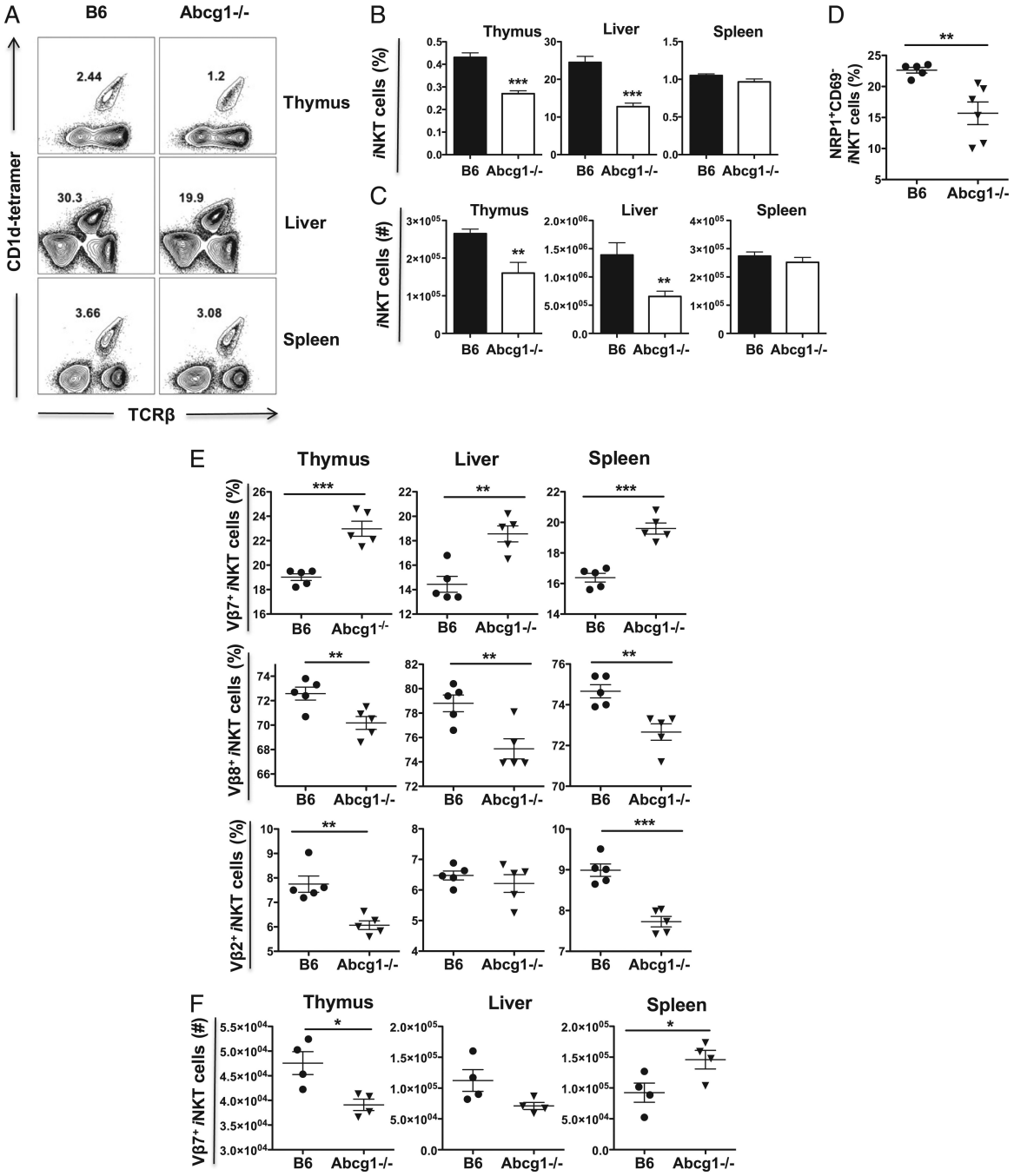


**FIGURE 1.**

*Abcg1*$^{-/-}$ mice display reduced *i*NKT cell frequencies in thymus and liver. (**A**) Thymocytes, liver mononuclear cells, and splenocytes from four- to six-week-old wild-type B6 and *Abcg1*$^{-/-}$ mice ($n = 9$) were stained with fluorophore-conjugated Abs and CD1d tetramer. Representative contour plots show CD19$^{-}$, CD8α$^{-}$, TCRβ$^{+}$, CD1d-tetramer$^{+}$ *i*NKT cells. Bar graphs show (**B**) frequency and (**C**) total cell number of *i*NKT cells in thymus, liver, and spleen (*i*NKT cells [%]: % of live cells). Data are pooled from two to three independent experiments (three to five mice per group for each experiment) with similar results. (**D**) Graph shows the frequency of NRP-1$^{+}$, CD69$^{-}$ *i*NKT cells in spleen. Representative data of two independent experiments with four-week-old mice (five to six mice per group) are

shown. (**E**) Thymocytes, liver mononuclear cells, and splenocytes from B6 ($n = 5$) and *Abcg1*$^{-/-}$ mice ($n = 5$) were stained with fluorophore-conjugated CD19, CD8α, TCRβ, Vβ7, Vβ8.1/2, and Vβ2 Abs, and CD1d tetramer, and analyzed by flow cytometry. Graphs show frequencies of Vβ7$^{+}$ (*top*), Vβ8.1/2$^{+}$ (*middle*), and Vβ2$^{+}$ (*bottom*) B6 and *Abcg1*$^{-/-}$ *i*NKT cells in thymus, liver, and spleen. (**F**) Graphs show absolute cell numbers of Vβ7$^{+}$ B6 ($n = 4$) and *Abcg1*$^{-/-}$ ($n = 4$) *i*NKT cells in thymus, liver, and spleen. Data are representative of two independent experiments. Error bars represent means ± SEM. Asterisks denote the significance of differences between groups (*$p < 0.05$, **$p < 0.01$, ***$p < 0.001$, two-tailed Student *t* test).

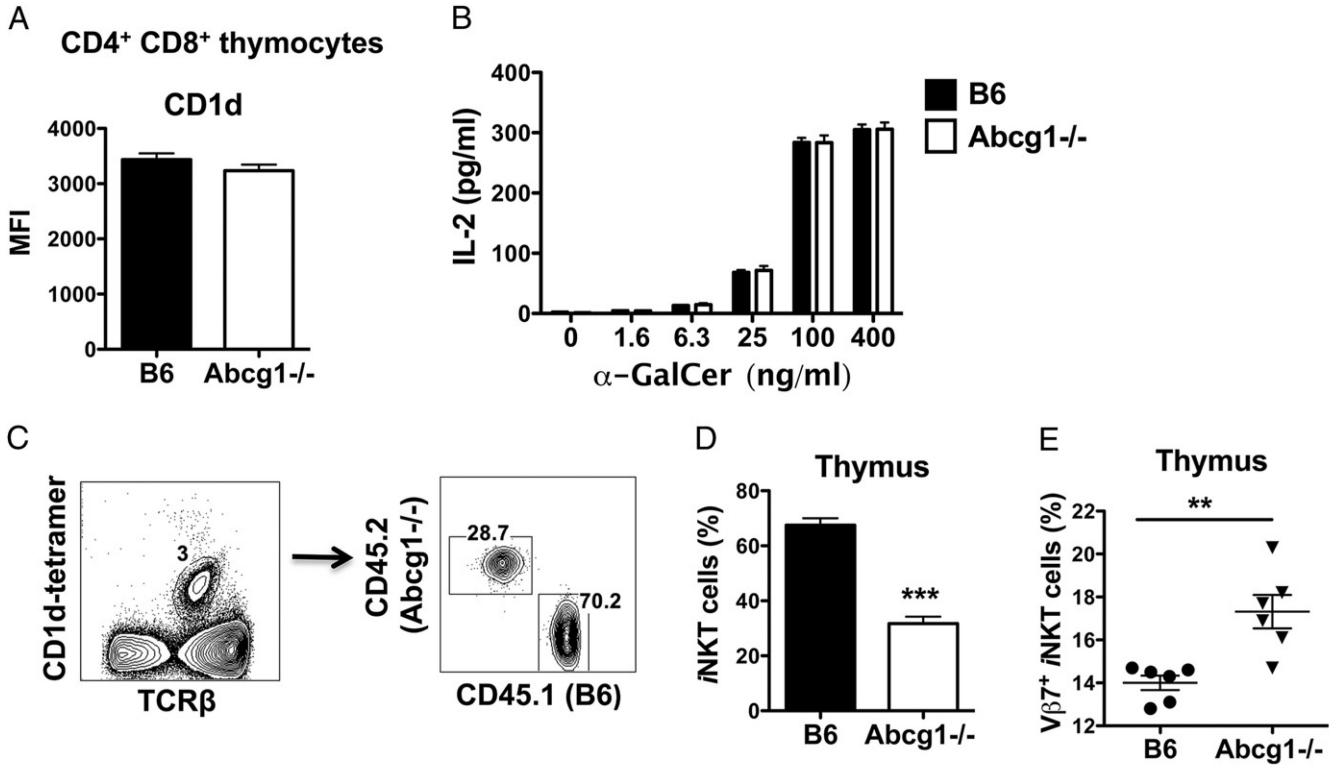


**FIGURE 2.**

ABCG1 deficiency affects *i*NKT cell development via a cell-intrinsic mechanism. (**A**) Thymocytes from B6 mice ($n = 5$) and *Abcg1*$^{-/-}$ mice ($n = 4$) were stained with CD4, CD8α, and CD1d Abs and analyzed by flow cytometry. Bar graph shows mean fluorescence intensity (MFI) of CD1d on CD4$^{+}$CD8$^{+}$ thymocytes from B6 and *Abcg1*$^{-/-}$ mice. Data are representative of two independent experiments with similar results. (**B**) *i*NKT cell hybridoma DN3A4-1.2 cells were cocultured with thymocytes from either B6 ($n = 4$) or Abcg1$^{-/-}$ ($n = 4$) mice in the presence of titrated amounts of α-GalCer in vitro. After 18 h, IL-2 production was detected by ELISA. Data are representative of two independent experiments with similar results. (**C** and **D**) Bone marrow chimeras were generated by reconstituting irradiated Rag1$^{-/-}$ mice ($n = 11$) with 1:1 mixed bone marrow cells from CD45.1$^{+}$ B6.SJL and CD45.2$^{+}$ *Abcg1*$^{-/-}$ donor mice. Single-cell suspension from thymus was analyzed by flow cytometry 12 wk following reconstitution. (C) Representative contour plots show CD19$^{-}$, CD8α$^{-}$, TCRβ$^{+}$, CD1d-tetramer$^{+}$ *i*NKT cells, which are gated on CD45.1$^{+}$ and CD45.2$^{+}$ to identify *Abcg1*$^{+/+}$ B6.SJL and *Abcg1*$^{-/-}$ *i*NKT cells, respectively. (D) Bar graph shows percentages of *Abcg1*$^{+/+}$ B6.SJL and *Abcg1*$^{-/-}$ *i*NKT cells in thymus. Data are pooled from three independent experiments (three to four mice per group for each experiment) with similar results. (**E**) Graph shows frequency of Vβ7$^{+}$ CD45.1$^{+}$ B6 and CD45.2$^{+}$ *Abcg1*$^{-/-}$ *i*NKT cells in thymus. Data are pooled from two independent experiments (three mice per group for each experiment) with similar results (**$p < 0.01$, ***$p < 0.001$).

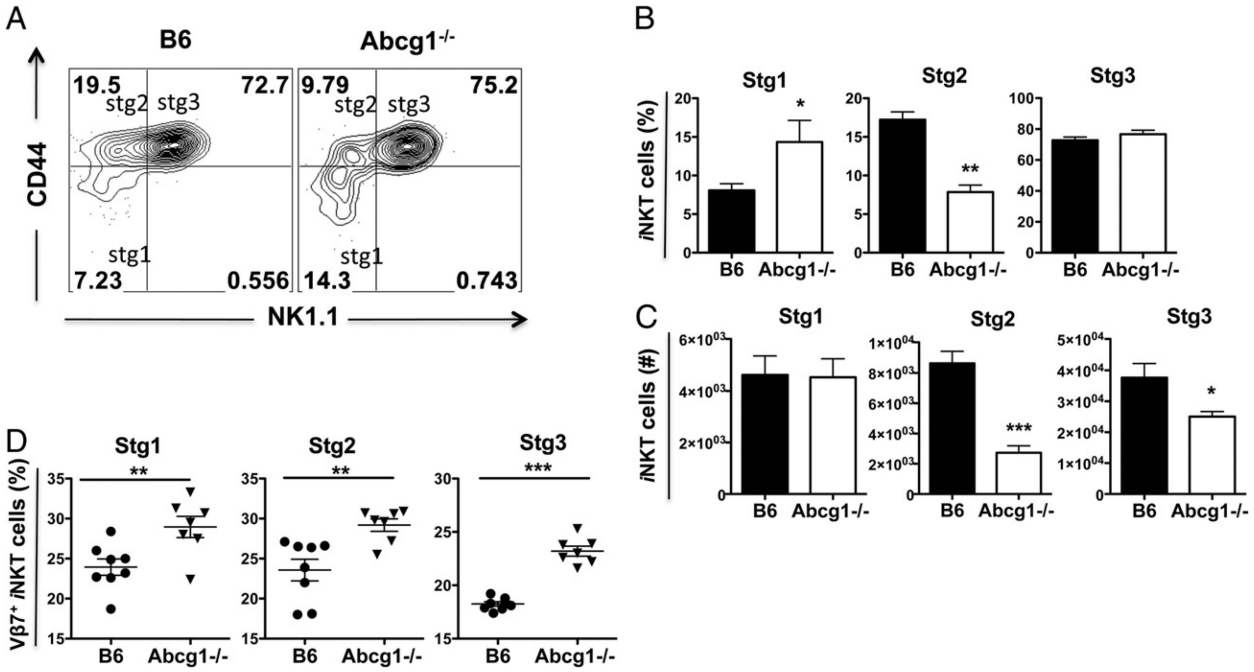


**FIGURE 3.**

ABCG1 deficiency affects the maturation of *i*NKT cells in thymus. Single-cell suspensions from thymi of B6:*Abcg1*$^{-/-}$ 1:1 mixed chimeric mice ($n = 10$) were stained with fluorophore-conjugated CD45.1, CD45.2, TCRβ, CD44, NK1.1 Ab, and CD1d tetramer and analyzed by flow cytometry. TCRβ$^{+}$ and CD1d-tetramer$^{+}$ cells were further gated to distinguish stage 1 (stg1, CD44$^{low}$ NK1.1$^{-}$), stage 2 (stg2, CD44$^{high}$ NK1.1$^{-}$), and stage 3 (stg3, CD44$^{high}$ NK1.1$^{+}$) *i*NKT cells. (**A**) Representative contour plots. Bar graphs show (**B**) percentages and (**C**) absolute cell numbers of CD45.1$^{+}$ B6 and CD45.2$^{+}$ *Abcg1*$^{-/-}$ *i*NKT cells of indicated maturation stages. Results are representative of two independent experiments with similar results. (**D**) Graphs show frequencies of Vβ7$^{+}$ thymic *i*NKT cells at stage 1–3 in B6 ($n = 8$) and Abcg1$^{-/-}$ ($n = 7$) mice. Data are pooled from two independent experiments (three to four mice per group for each experiment) with similar results (*$p <$ 0.05, **$p < 0.01$, ***$p < 0.001$).

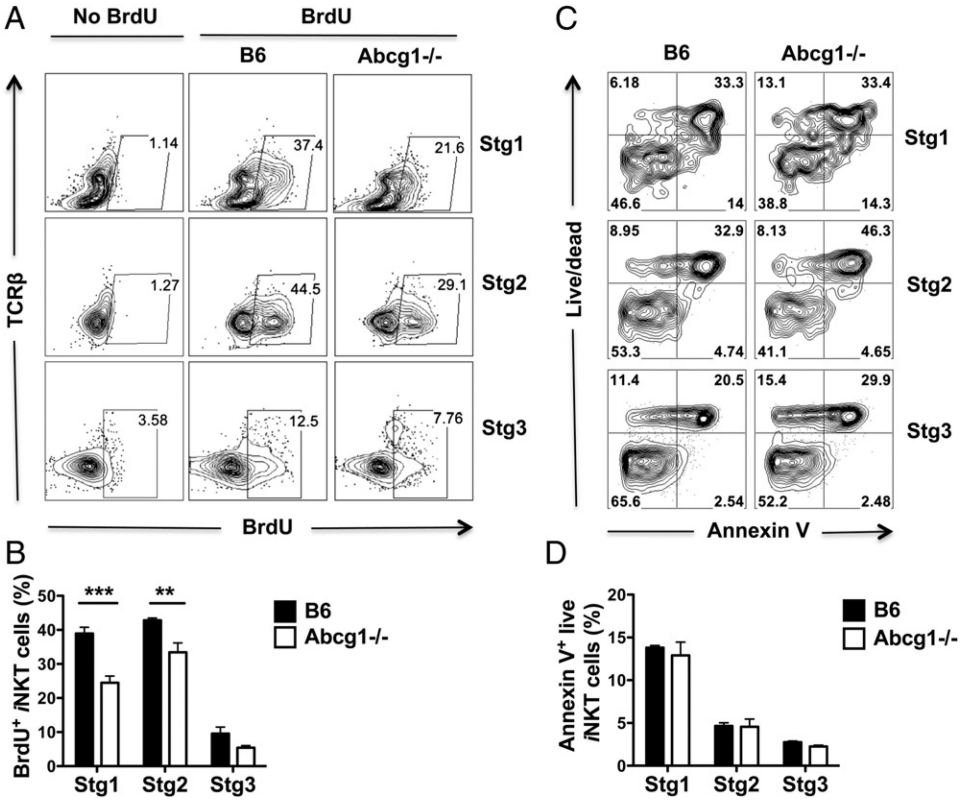


**FIGURE 4.**

*Abcg1*$^{-/-}$ *i*NKT cells display reduced proliferation in early stages of development. B6 (n = 7) and *Abcg1*$^{-/-}$ ($n = 8$) mice were injected with BrdU three times every 4 h. The next day, thymi were harvested and single-cell suspensions were stained with fluorophore-conjugated CD8α, TCRβ, CD44, NK1.1, BrdU Ab, and CD1d tetramer and analyzed by flow cytometry. TCRβ$^{+}$ and CD1d-tetramer$^{+}$ cells were further gated to distinguish stage 1 (stg1, CD44$^{low}$ NK1.1$^{-}$), stage 2 (stg2, CD44$^{high}$ NK1.1$^{-}$), and stage 3 (stg3, CD44$^{high}$ NK1.1$^{+}$) *i*NKT cells. (**A**) Representative contour plots and (**B**) bar graphs show BrdU incorporation by *i*NKT cells at each stage. Data are pooled from two independent experiments (three to four mice per group for each experiment) with similar results. (**C** and **D**) Thymocytes from B6 ($n = 3$) and *Abcg1*$^{-/-}$ ($n = 3$) mice were cultured overnight and the next day stained with fluorophore-conjugated CD8α, TCRβ, CD44, NK1.1, annexin V Ab, CD1d tetramer, and a live/dead marker and analyzed by flow cytometry. (C) Representative contour plots and (D) bar graphs show percentages of apoptotic (annexin V$^{+}$ live) *i*NKT cells at stage 1–3. Data are representative of two independent experiments with similar results (**$p < 0.01$, ***$p < 0.001$).

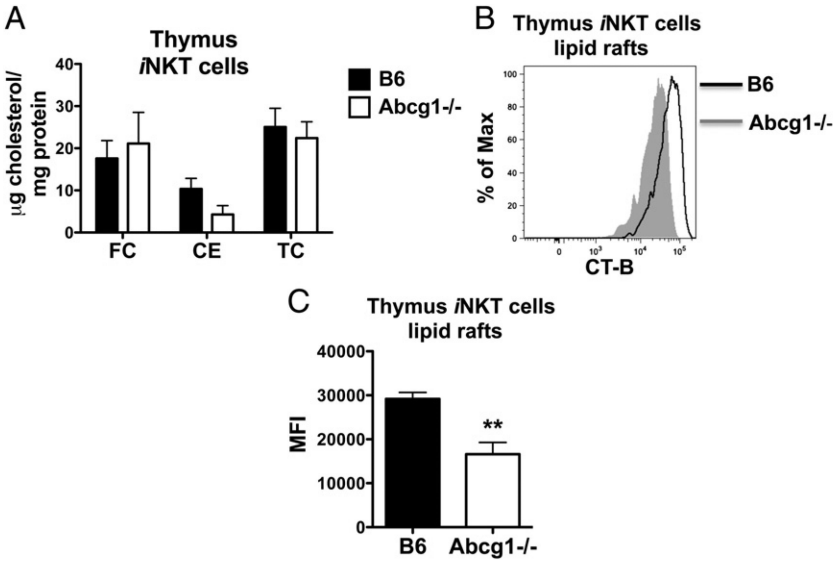


**FIGURE 5.**

*Abcg1*$^{-/-}$ *i*NKT cells display no change in cholesterol content, but have lower lipid raft content. (**A**) *i*NKT cells were FACS sorted from thymus of B6 and *Abcg1*$^{-/-}$ mice ($n = 9$; 27 mice, 3 mice were pooled for each sample per group), and free cholesterol (FC), cholesteryl ester (CE), and total cholesterol (TC) were measured by gas chromatography. Data are pooled from three independent experiments (3 samples per group for each experiment) with similar results. (*B* and *C*) Thymocytes from B6 ($n = 4$) and *Abcg1*$^{-/-}$ ($n = 4$) mice were stained with fluorophore-conjugated Abs, CD1d tetramer, and CT-B, and analyzed by flow cytometry. (B) Representative plot shows lipid raft staining (CT-B) of *i*NKT cells in thymus. (C) Graph shows mean fluorescence intensity (MFI) of CT-B of *i*NKT cells in thymus. Data are representative of two independent experiments with similar results (**$p < 0.01$).

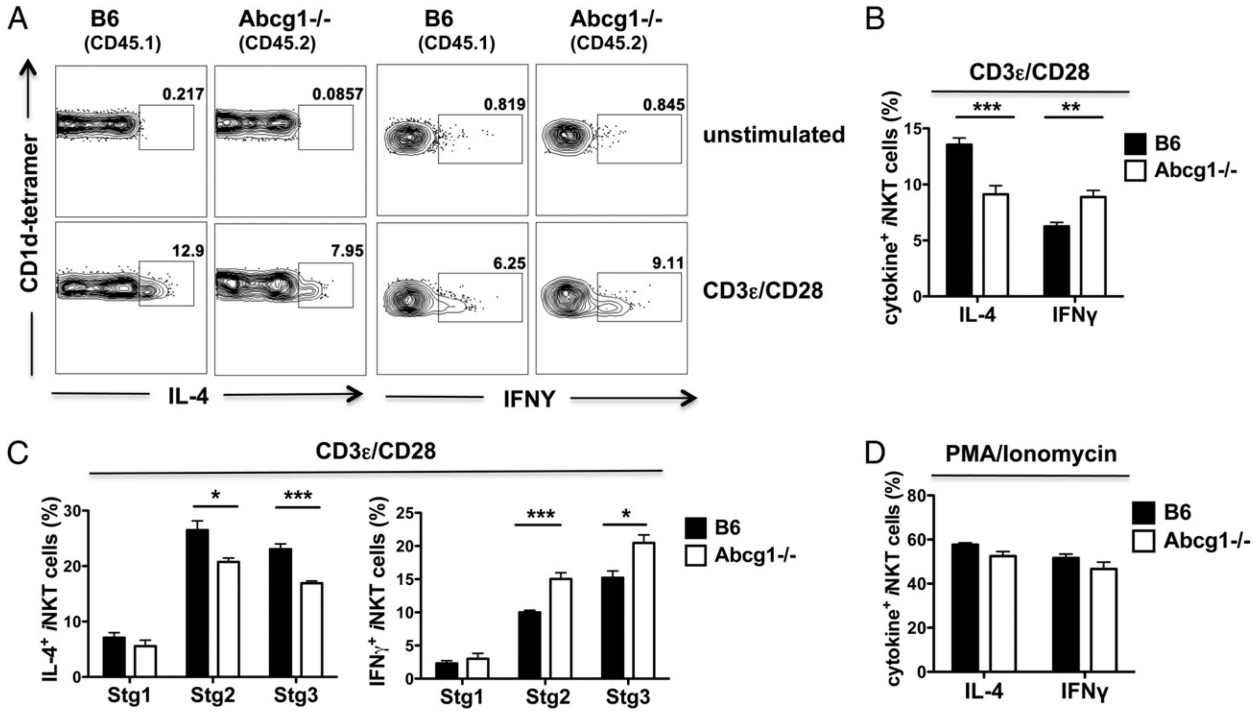


**FIGURE 6.**

*Abcg1*$^{-/-}$ *i*NKT cells display reduced IL-4 and increased IFN-γ production following TCR-driven activation. (**A** and **B**) Thymocytes from B6:*Abcg1*$^{-/-}$ 1:1 mixed chimeric mice ($n$ = 8) were stimulated with plate-bound αCD3ε and soluble αCD28 Ab for 4 h in vitro and stained with fluorophore-conjugated surface Abs and CD1d tetramer, followed by intracellular staining with IL-4 and IFN-γ Ab, and analyzed by flow cytometry. (A) Representative contour plots and (B) bar graph show percentages of IL-4– and IFN-γ–producing CD45.1$^{+}$ B6 and CD45.2$^{+}$ *Abcg1*$^{-/-}$ *i*NKT cells based on CD8$^{-}$, TCRβ$^{+}$, CD1d-tetramer$^{+}$ gating. Data are pooled from two independent experiments (4 mice per group for each experiment) with similar results. (**C**) Thymocytes from B6 ($n$ = 4) and *Abcg1*$^{-/-}$ ($n$ = 4) mice were stimulated with aCD3ε/αCD28 Abs and analyzed, as described above. Bar graphs show IL-4 (*left*) and IFN-γ (*right*) producing stage 1 (stg1, CD44$^{low}$ NK1.1$^{-}$), stage 2 (stg2, CD44$^{high}$ NK1.1$^{-}$), and stage 3 (stg3, CD44$^{high}$ NK1.1$^{+}$) *i*NKT cells. (**D**) Thymocytes from B6 ($n$ = 4) and *Abcg1*$^{-/-}$ ($n$ = 4) mice were stimulated with PMA/ionomycin for 4 h in vitro and stained with fluorophore-conjugated surface Abs and CD1d tetramer, followed by intracellular staining with IL-4 and IFN-γ Ab, and analyzed by flow cytometry. Bar graph shows percentages of IL-4– and IFN-γ–producing *i*NKT cells based on CD8$^{-}$, TCRβ$^{+}$, CD1d-tetramer$^{+}$ gating. Data are representative of two independent experiments with similar results (*β < 0.05, **$p$ < 0.01, ***$p$ < 0.001).